ACS Catalysis

RESEARCH ARTICLE

pubs.acs.org/acscatalysis

High-Throughput Discovery and Optimization of Hafnium Heteroaryl-amido Catalysts for the Isospecific Polymerization of Propylene

Gary M. Diamond,[‡] Keith A. Hall, Anne M. LaPointe,[*,†] Margarete K. Leclerc,[∥] James Longmire,[‡] James A. W. Shoemaker,[‡] and Pu Sun[§]

Symyx Technologies, Inc., 3100 Central Expressway, Santa Clara, California 95051, United States

Supporting Information

ABSTRACT: New nonmetallocene catalysts for the isospecific polymerization of propylene were discovered using high-throughput screening. These hafnium heteroaryl-amido catalysts are structural analogues of the highly successful hafnium pyridyl-amido catalysts. Initial primary and secondary screening of a library of five thiazole-amine ligands with Zr and Hf with propylene resulted in the discovery of highly active catalysts with high activity, high molecular weight capability, and stereoinduction that ranged from low to high, depending on the ligand and activation conditions. Subsequent screening revealed that bulky aryl substituents at the N-aryl (R1), thiazole *ortho* position (R2) and the bridge position (R3) were preferred for high activity, although stereoinduction was lower than that observed for the pyridyl-amidos. The thiazole-amine catalysts containing a 2-methoxyphenyl substituent at R2 and activation conditions that included $B(C_6F_5)_3$ formed highly isotactic polypropylene with low catalyst activity. Subsequent complexation and reactivity studies revealed that in the presence of $B(C_6F_5)_3$ and trialkylaluminum reagent, demethylation of the bound ligand ether occurred, resulting in binding of the ligand in a tridentate [O^-, N, N^-] fashion. The resulting thiazole-amido phenoxide complex was prepared independently and is a highly stereospecific catalyst for the polymerization of propylene, although it exhibited low activity relative to the other thiazole-amido catalysts. This structural clue suggested that expansion of the ring formed upon orthometalation at the R2 position might be advantageous for stereocontrol. A library of imidazole-amine and thiazole-amines containing 2-methylbenzothiophene (2-MeBZT) and 2-ethylbenzofuran substituents (2-EtBZF) at R2 was prepared, complexed to Hf, and screened with propylene at 110 °C. Many of the catalysts showed high activity, high molecular weight capability, and very good stereoinduction.

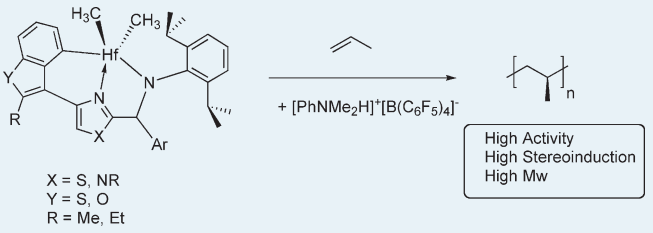

KEYWORDS: olefin polymerization, group 4 transition metal complexes, nonmetallocene catalysts, isotactic polypropylene, hafnium pyridyl-amido complexes, high-throughput experimentation

INTRODUCTION

The development of single-site catalysts for olefin polymerization has been the subject of intensive research over the past 30 years.[1,2] Large advances have been made possible by the discovery of alumoxanes and well-defined noncoordinating activators (NCAs).[3−6] The use of NCAs has greatly facilitated detailed mechanistic studies, allowing the activation, propagation, and deactivation steps to be studied. Modern NMR methods, such as stopped-flow measurements, have also been utilized to study the polymerization.[7] At the same time, substantial advances in ligand design were facilitated by both an improved mechanistic understanding and advances in organic synthesis.[8−10] This has resulted in the development of new classes of catalysts and the discovery of some unprecedented polymer architectures, including novel microstructures,[11] tandem catalysis,[12,13] and incorporation of polar functionalities.[14] Initial efforts focused largely on metallocenes and half-metallocenes, but a number of highly active nonmetallocene catalysts have been reported in the last 15 years. These include both Group 4[15−24] and late metal polymerization catalysts.[25−29] During this time, Symyx pioneered the development of high-throughput synthesis and screening techniques for use in homogeneous catalyst research.[30−32] This has permitted the discovery of several new classes of olefin polymerization catalysts, including a class of hafnium catalysts for the isospecific polymerization of propylene.[33−36]These catalysts (Figure 1) contain a pyridyl-amine ligand, which is readily amenable to introduction of a diverse array of substituents on the ligand framework. The aryl substituent on the pyridyl ring undergoes metalation during the course of complexation.

With the proper choice of substituents, the hafnium pyridyl-amido catalysts exhibit an unprecedented combination of activity, isospecificity, and high molecular weight capability at high polymerization temperatures, and produce polypropylene with an unusual microstructure.[37−40]Additionally, these catalysts have found use in a novel chain shuttling catalyst system.[41,42]

Received: April 7, 2011
Revised: June 4, 2011
Published: June 27, 2011

The activation and polymerization mechanism has been the subject of recent detailed studies (Scheme 1).[43−46]

Mechanistic evidence suggests that upon activation with a proton source such as $[PhNMe_2H]^+[B(C_6F_5)_4]$ (ABF_{20}) the Hf-aryl bond is cleaved (**1c**), followed by reorthometalation with loss of methane to yield a monomethyl cation (**1d**), which subsequently inserts 1 equiv of propylene into the *Hf-aryl bond* (**1e**). This seven-member metallacycle species is proposed to be the active species in the polymerization, with the polymer chain growth occurring at the alkyl group rather than on the metallacycle. Although the pyridyl-amido catalysts possess a chiral center at the bridge position (R3), and stereoselectivity increases as the steric bulk of aryl substituents at R3 is increased, recent work by Coates et al. suggests that the geometry of the expanded metallacycle also influences the stereocontrol.[47,48] C_s-symmetric achiral pyridyl-amidos produce polypropylene and poly-1-hexene with predominantly isotactic microstructures at ambient temperatures (Scheme 2). These results are consistent with the insertion of olefin into the metal-aryl bond to form a catalyst that does not have C_s symmetry. Consistent with these results, model complexes with a preformed 6-member metallacycle (generated from intramolecular 2,1 insertion of a vinyl moiety) also were active polymerization catalysts and produced isotactically enriched polypropylene.[47,48] These results suggest that both a chiral center at R3 and the expanded metallacycle can promote stereoselectivity.

We were interested in whether other classes of heteroaryl-amine ligands would be useful for olefin polymerization. These include thiazole-amines, imidazole-amines, oxazole amines, and oxadiazole-amines (Figure 2). The discovery and optimization of hafnium thiazole- and imidazole-amido catalysts will be reported here.[49,50]

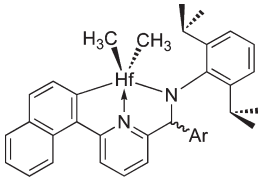

Figure 1. Orthometalated hafnium pyridyl-amido precatalyst.

RESULTS AND DISCUSSION

Primary Screening Discovery Experiments. The strategies and methodologies used within the Symyx primary screen have been discussed previously.[30,33] Five examples of thiazole-amine ligands (Figure 3) were prepared and studied in our high-throughput propylene primary screen as part of a larger array of ligands. Each ligand was screened under 24 unique complexation-activation conditions with Ti, Zr, and Hf. Complexation-activation conditions probed include metal precursor identity, metal:ligand ratio, Al reagent identity, and activator identity.

Table 1 displays the range of yields for **2a**−**e** with Hf under various complexation-activation conditions (14 examples per ligand). Yields ranged from 1 to 190 mg. Similar results were obtained for L/M ratios of 2:1 and 1:1. The combination of ligands **2a**, **2d**, or **2e** with Hf all produced polymers whose FT-IR indices ranged from atactic (0.20) to moderately isotactic (0.50) polypropylene. For each of these ligands, the choice of metal precursor and activation conditions had little effect on the tacticity indices (method error ±0.05). In contrast, **2b** and **2c** exhibited an inverse correlation between yield and FT-IR index, with particularly low yields and higher FT-IR indices observed

Scheme 1. Proposed Activation Mechanism for Hafnium Pyridyl-Amido Catalysts

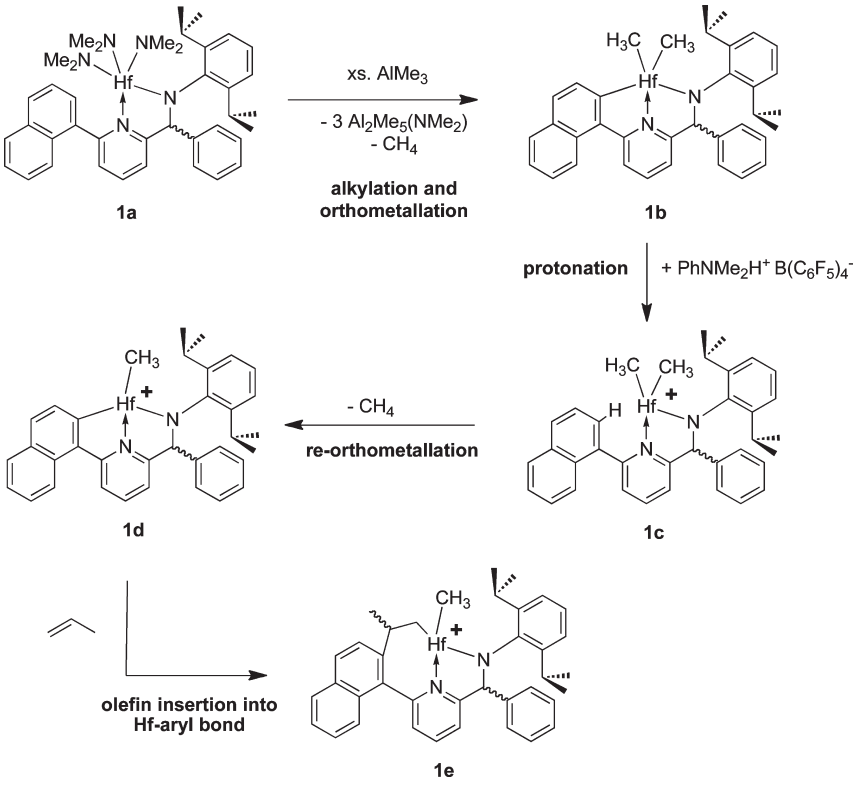

dx.doi.org/10.1021/cs200180x |ACS Catal. 2011, 1, 887–900

when a combination of MBn_4 and $B(C_6F_5)_3$ (BF_{15}) is used as the activator.

Selected ligand−metal-activator combinations were then screened on a larger scale in the Symyx PPR at 75 °C using in situ complexation with $M(NMe_2)_4$ and MBn_4 (M = Zr, Hf). The results are shown in Figure 4. As can be seen, activity was somewhat higher on average for Hf than for Zr. Metal−ligand combinations of ligands **2a**, **2d**, and **2e** show high polymerization activity (A > 500 mg/ (μmol catalyst min)) under some complexation and activation conditions. The range of FT-IR indices observed is fairly narrow for each ligand−metal combination and is slightly higher for Hf than Zr. Polymer molecular weights for these catalysts systems varied depending on the activation condition, but were >100k, with many examples above 500k. In contrast, catalysts generated from ligands **2b** and **2c** show lower activity and a much wider range of FT-IR indices. The polymers formed by these metal−ligand combinations ranged from atactic (FT-IR < 0.30) to relatively isotactic (FT-IR > 0.6). The combination of **2c**, $ZrBn_4$, and alkylator/activator combinations that included BF_{15} and AlR_3 exhibited very low activity, but the resulting polymer had the highest

Scheme 2. Preparation of Isotactically-Enriched Polypropylene by Pyridyl-Amido Catalysts Lacking Bulky Aryl Substituents at R3

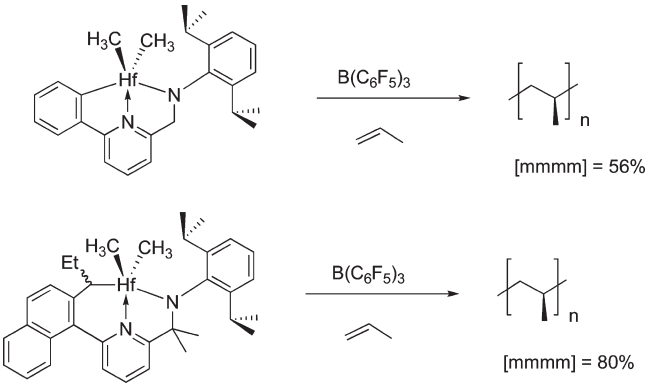

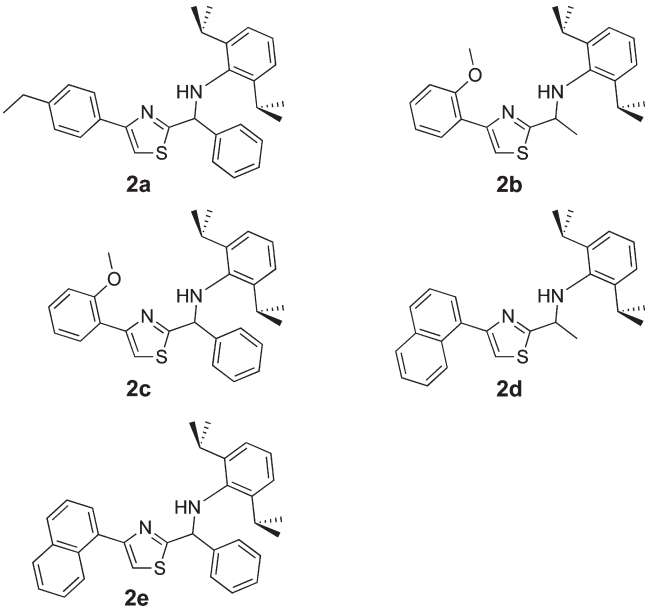

Figure 3. Thiazole-amine ligands in the first primary screening library.

Table 1. Polypropylene Yield and FT-IR Data from Library 1[a]

ligand	yield (mg)	FT-IR
2a	17−190	0.33−0.48
2b	1−132	0.20−0.38
2c	2−61	0.20−0.82
2d	1−160	0.22−0.32
2e	3−137	0.33−0.69

[a] Complexed with $Hf(NMe_2)_4$ and $HfBn_4$. Polymerization conditions: 75 °C, 80 psi C_3H_6, toluene.

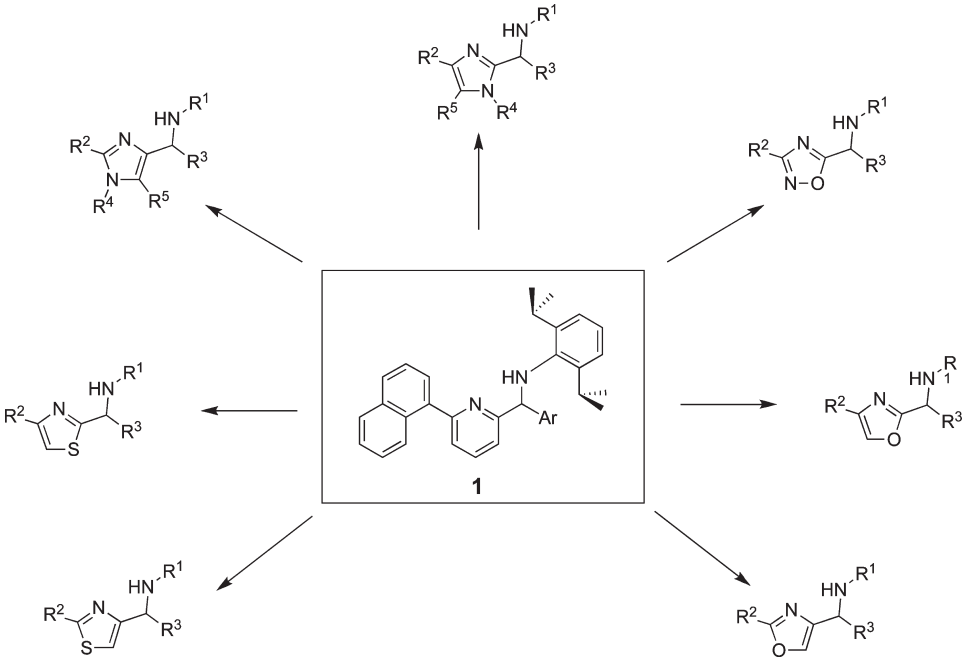

Figure 2. Examples of heteroaryl-amine ligands.

dx.doi.org/10.1021/cs200180x |ACS Catal. 2011, 1, 887–900

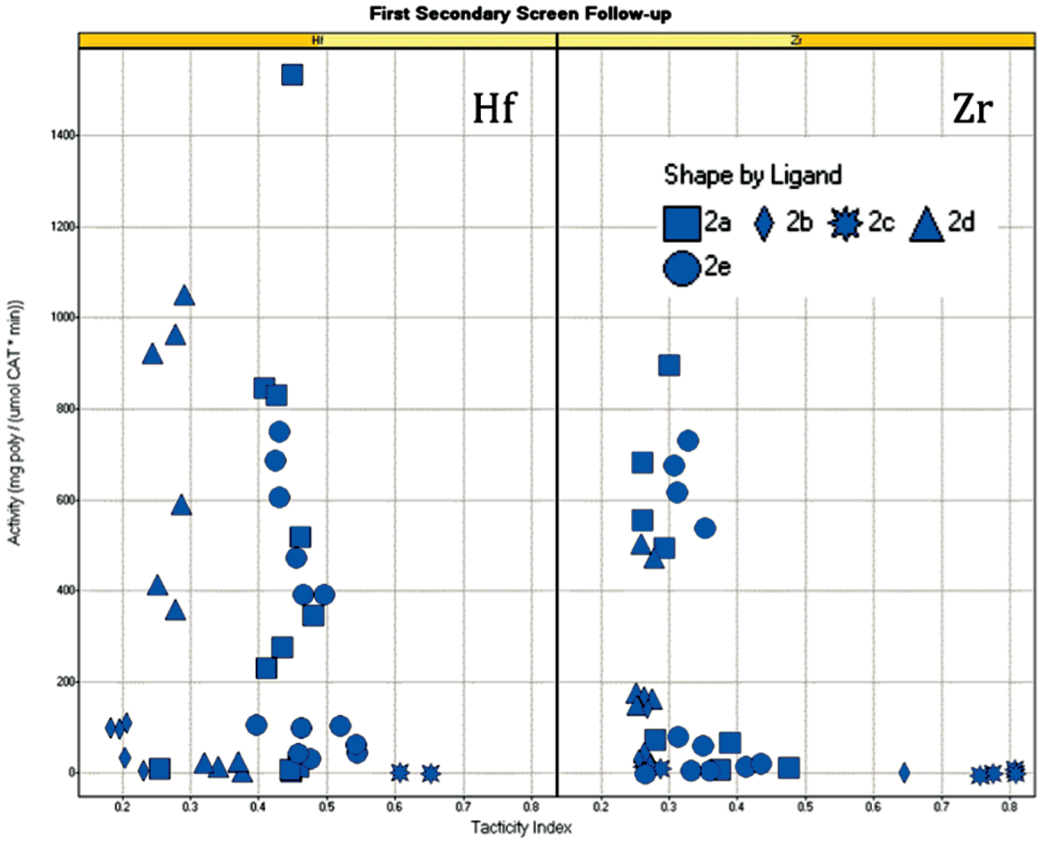

Figure 4. Secondary screening activity and FT-IR data for ligands **2a**−**e**/M (M = Zr, Hf).

crystallinity for this round of screening. This is consistent with the results from the primary screening.

Because of the combination of high activity, extremely high molecular weight, and moderate stereocontrol, the thiazole-amines were a very promising new lead. For this reason, a systematic study of ligand substituent effects was performed.

Second Thiazole-Amine Library. Prior studies with pyridyl-amines showed that catalyst performance is very dependent on the steric properties of R1, R2, and R3 (Figure 2).[33] 23 new thiazole-amines were prepared and screened in the PPR at 75 °C under a variety of complexation and activation conditions. Data from **2e** is included as a reference. The R1 and R3 variations tested are shown in Figure 5. R2 was held constant (R2 = 1-napthyl), and R1 and R3 were varied systematically.

For Library 2, the activity and FT-IR data for Hf are shown in Figure 6 and 7, respectively. Several trends were observed. For the active systems, the resulting polymer has M_w 400−1000k. When R2 and R3 were held constant, the ligands containing 2,6-di-*iso*propyl (DIP) substitution on the phenyl ring showed higher activity than the other derivatives. When R3 is an alkyl group, higher activity and FT-IR indices are observed as the steric bulk is increased from primary (R = CH_3, CH_2Ph) to secondary (cyclohexyl, di-*iso*propyl), but no polymer was produced when R3 = *t*-Bu. A similar trend is observed for the series containing aryl substituents at R3, with the highest tacticity resulting when R3 = mesityl (**3**). This system also showed the highest activity, with an activity of almost 5000 mg/(μmol catalyst min) under certain activation conditions.

For comparison, the pyridyl-amido complex **1a** has an activity of about 700 under similar in situ screening conditions.[33] The results of this SAR study suggested that steric bulk at R3 results in increasing catalyst activity and improved tacticity in the resulting polymer. However, none of the catalysts produced polymer with crystallinity as high as that produced by **2c**/M (M = Zr, Hf) or the optimized pyridyl amines. Thus, it was necessary to study the organometallic chemistry of the Group 4 thiazole-amido complexes to gain insight into ways to further optimize these interesting catalysts.

Complexation Studies. Initially, we focused on the metal−ligand combinations that resulted in the highest activity (Hf + **3**) or tacticity indices (Zr + **2c**) in the first two rounds of screening and investigated the complexation reactions under similar conditions to those used for in situ screening.

Reaction of 1 equiv of $Hf(NMe_2)_4$ with **3** in toluene for 2 d at 110 °C yields the colorless tris-amido complex **4** in 77% yield. (eq 1). No evidence of orthometalation is observed under the synthesis conditions.

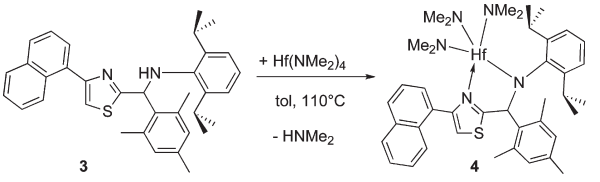

(1)

Alkylation of the tris(amido) complex with excess Al_2Me_6 results in formation of the colorless trimethyl complex **5** in 60% yield (eq 2). Unlike the pyridyl-amido methyl complexes,[33] **5**

dx.doi.org/10.1021/cs200180x |*ACS Catal.* 2011, 1, 887–900

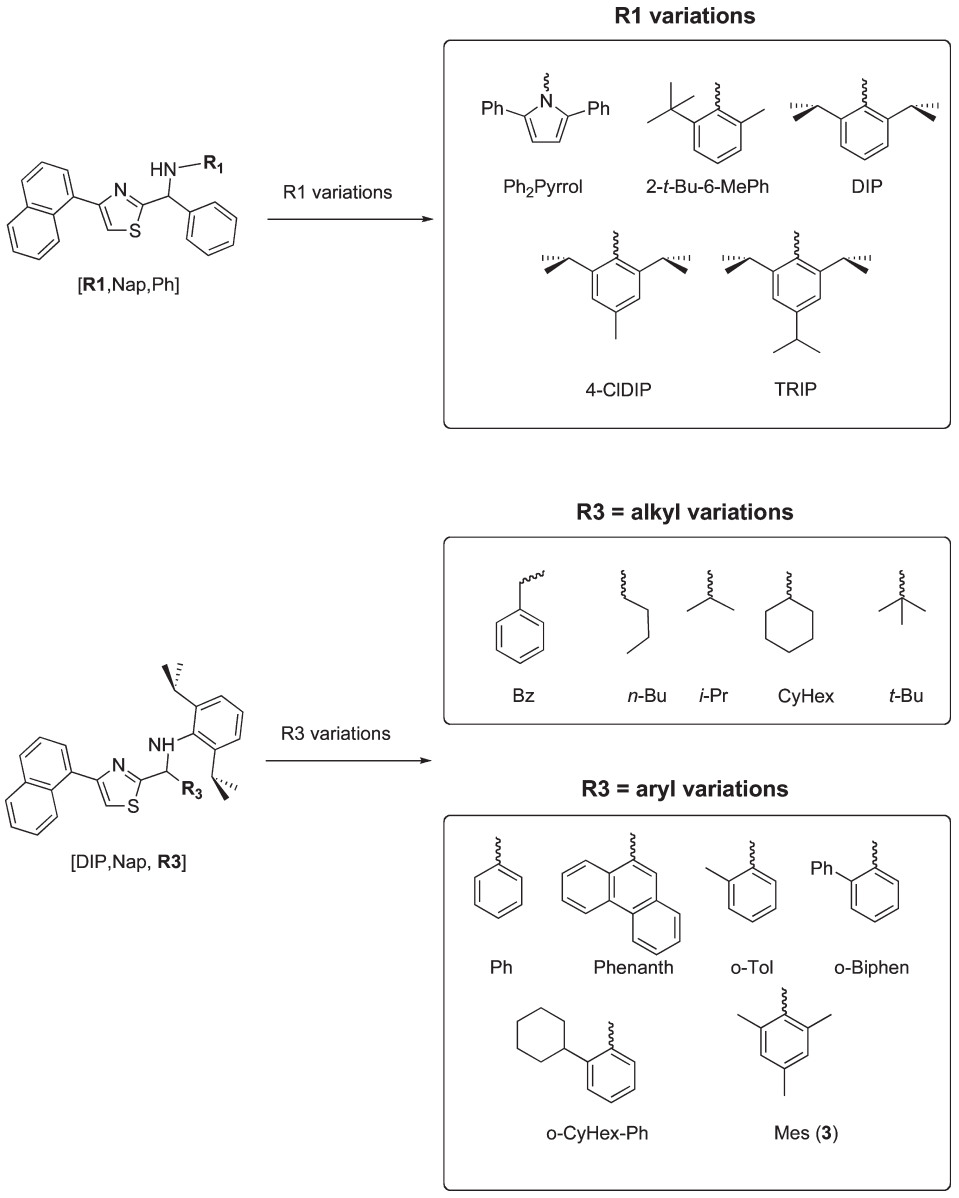

Figure 5. Second thiazole-amine screening library.

does not undergo orthometalation at ambient conditions, although it does occur at 70 °C in toluene.

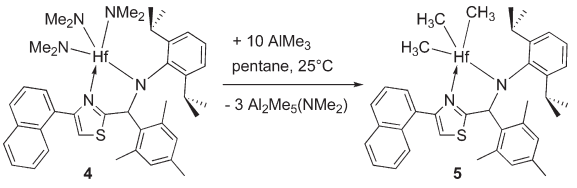

(2)

The structures of complexes **4** and **5** were solved by X-ray structure determination. The structures are shown in Figure 8 and 9, respectively. Both structures have a distorted trigonal bipyramidal geometry, with the thiazole imine nitrogen bound to Hf. The trimethyl complex, **5** is somewhat more distorted than the tris(amido) analogue **4**. For the tris(amido) complex, **4**, the Hf−N imine (2.49 Å) and Hf−NAryl (2.14 Å) bond distances were similar to those observed in a Hf pyridyl-amido tris-(dimethyl amido) complex (2.51 Å and 2.09 Å).[33]

The system that gave the highest tacticity polymer, **2c**/$ZrBn_4$, was also investigated. The reaction of **2c** with $ZrBn_4$ in toluene at 75 °C for 5 h results in formation of 2 equiv of toluene and a yellow complex, **6**, whose ^{1}H NMR is consistent with the orthometalated dibenzyl complex (eq 3). No intermediate species are observed.

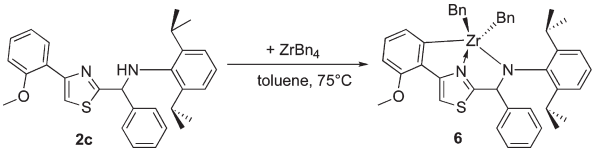

(3)

In contrast, when **2c** is reacted with the zwitterionic complex $[ZrBn_3][BnB(C_6F_5)_3]$[51,52] or a combination of $ZrBn_4$ and BF_{15}

dx.doi.org/10.1021/cs200180x |ACS Catal. 2011, 1, 887–900

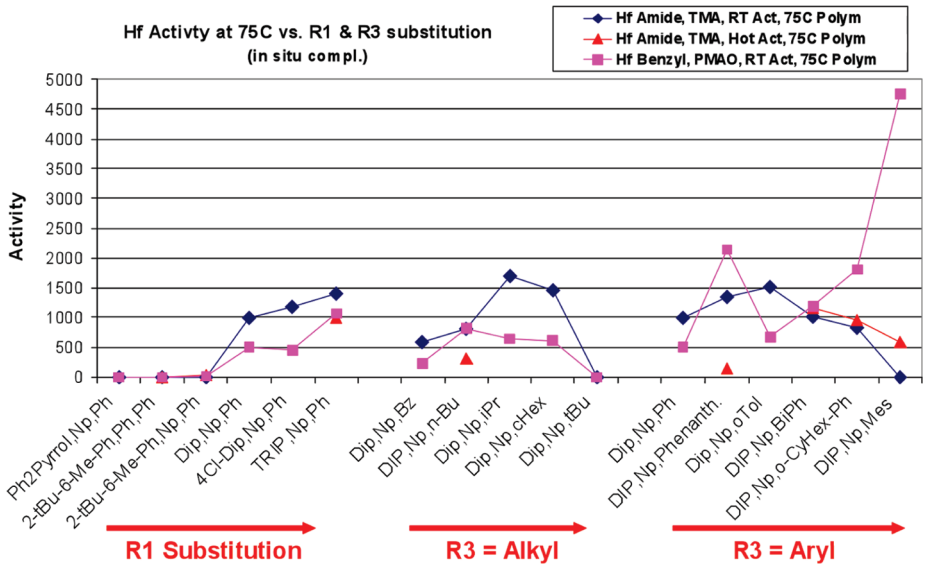

Figure 6. Effect of thiazole-amine substituents on polymerization activity (activity = mg polymer/(μmol catalyst min)).

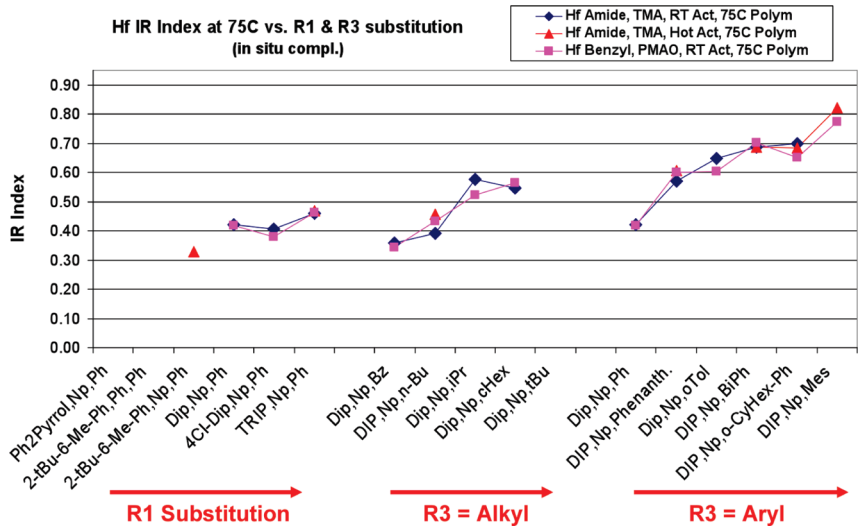

Figure 7. Effect of thiazole-amine substituents on FT-IR index.

at room temperature, 1 equiv of toluene is formed, along with an orange complex, **7**, whose NMR is consistent with a zwitterionic dibenzyl complex (eq 4). The proposed structure is shown below.

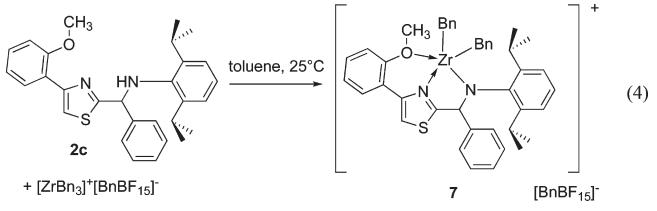

(4)

It should be noted that the typical complexation conditions for the in situ screening are 30 min at 75 °C, so when the BF_{15}/ABF_{20} activation conditions are used, formation of **6** is incomplete as measured by ^{1}H NMR and a sizable portion of **7** may form from unreacted **2c**/Zr/BF_{15}.

Complexes **4**−**7** were screened with propylene at 75 and 110 °C in the PPR under a range of activation conditions. Selected data is shown in Table 2. **4** and **5** showed high activity and similar tacticity and M_w trends, consistent with formation of a common intermediate. The activity is higher than was observed in the in situ complexation experiments; this is frequently observed for extremely bulky ligands which may not undergo complete complexation under the in situ screening conditions. Activity and M_w remained very high when the polymerization was conducted at 110 °C.

Complex **6** and **7** were screened under various activation conditions at 75 °C. **6** shows moderate activity (A = 150 mg/(μmol catalyst min)) and low stereoinduction. In contrast, **7** shows low activity (A = 14), but the resulting polymer has high

dx.doi.org/10.1021/cs200180x |*ACS Catal.* 2011, 1, 887–900

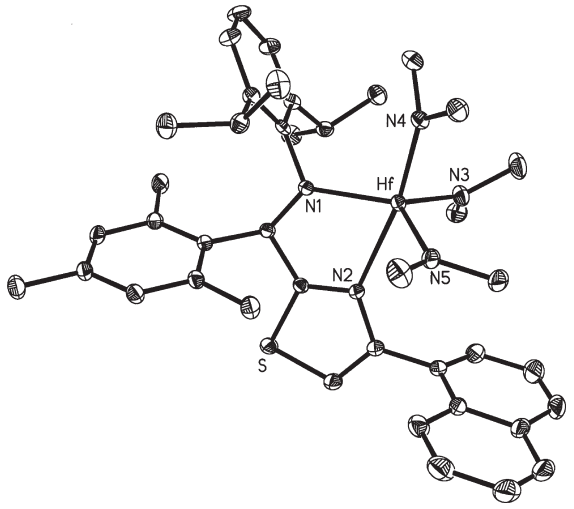

Figure 8. Molecular structure of **4** (hydrogen atoms omitted for clarity). (Selected Bond Lengths (Å) Hf−N(1) 2.14, Hf−N(2) 2.49, Hf−N(3) 2.06, Hf−N(4) 2.06, Hf−N(5) 2.04. Selected Bond Angles (deg) N(1)−Hf−N(2) 70.7, N(1)−Hf−N(4) 100.2, N(1)−Hf−N(3) 119.6, N(1)−Hf−N(5) 125.2, N(2)−Hf−N(4) 170.8, N(2)−Hf−N(3) 89.9, N(2)−Hf−N(5) 89.7, N(3)−Hf−N(4) 96.4, N(4)−Hf−N(5) 94.4, N(3)−Hf−N(5) 110.6).

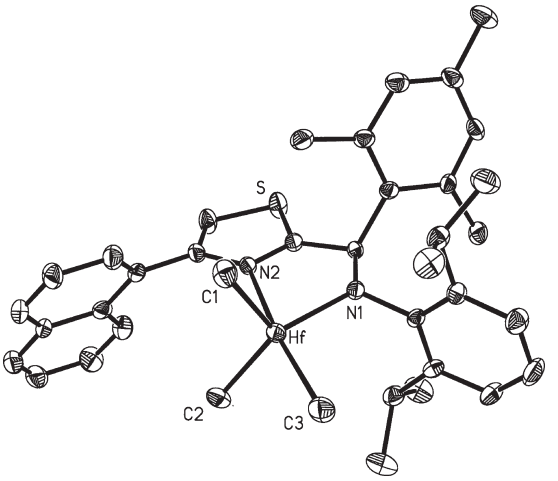

Figure 9. Molecular Structure of **5** (hydrogen atoms omitted for clarity). (Selected Bond Lengths (Å) Hf−N(1) 2.09, Hf−N(2) 2.46, Hf−C(1) 2.23, Hf−C(2) 2.22, Hf−C(3) 2.25. Selected Bond Angles (deg) N(1)−Hf−N(2) 71.2, N(1)−Hf−N(3) 100.0, N91)−Hf−C(2) 123.9, N(1)−Hf−C(1) 113.6, N(2)−Hf−C(3) 166.6, N(2)−Hf−C(2) 81.2, N(2)−Hf−C(1) 94.7, C(3)−Hf−C(2) 96.3, C(3)−Hf−C(1) 98.2, C(1)−Hf−C(2) 116.5).

crystallinity (FT-IR = 0.89, T_m =152 °C). Interestingly, the stereoinduction of the polymer formed was not influenced by the choice of activator, even though this had been observed for the in situ complexation experiments. The experimental evidence suggests that the structure of the precatalysts strongly influences the stereoselectivity of the resulting polymer, although it is possible to envision common intermediates formed in the activation of **6** and **7**.

At this point, we were beginning to suspect that the complexed ligand was being modified in situ by the alkylators and/or activators present. To test this hypothesis, a series of quenching experiments was performed and the organic products were analyzed by ^{1}H NMR and GC-MS. When **7** was treated with tri-isobutylaluminum (TIBA) or a combination of TIBA/ABF_{20} and then quenched, a new product was observed (eq 5). NMR and GC-MS data are consistent with demethylation of the methoxyphenyl moiety of the ligand, as shown. No demethylation is observed in the absence of TIBA.

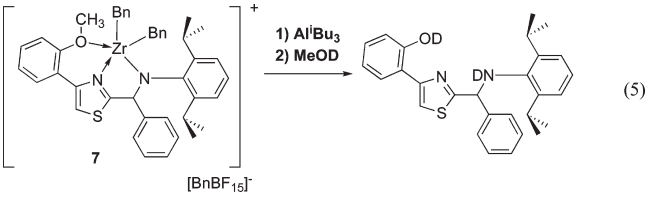

(5)

Demethylation of bound ethers has been reported in other group 4 complexes.[53] However, it could not be determined whether the demethylation was an unproductive side reaction or if the putative phenoxide complex was itself an active species. Thus, we attempted to prepare the isolated phenoxide complex in pure form and test its performance under identical reactor conditions.

The phenol thiazole-amine ligand was prepared by demethylation of ligand **2c**. For comparison purposes, a bulkier phenol thiazole-amine with a mesityl substituent at R3 was also prepared. The reaction of the free ligand (R3 = Ph) with 1 equiv of MBn_4 (M = Zr, Hf) results in formation of 2 equiv of toluene and the 5-coordinate complexes (**8a** M = Zr; **8b** M = Hf) (eq 6).

Table 2. Polymerization of Propylene by Complexes 4−7[a]

entry	complex	alkylator	activator	activity[b]	M_w(k)	FT-IR index	Mp (°C)
1[c]	**4**	10 TMA	ABF20	6810	1320	0.8	126
2[d]	**4**	10 TMA	ABF20	2290	520	0.78	121
3[d]	**5**	5 DIBAL	ABF20	2410	350	0.81	122
4[c]	**6**	5 TMA	2BF15/ABF20	150	370	0.28	n.d.
5[c]	7	5 TIBA	ABF20	14	360	0.89	152

[a] Toluene, 100 psi C_3H_6. [b] mg/(μmol catalyst*min). [c] 75 °C [d] 110 °C.

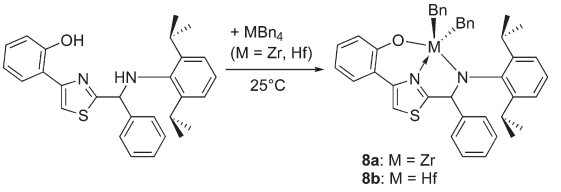

(6)

The ligand with R3 = mesityl did not react with MBn_4 at temperatures up to 75 °C, but the reaction with 1 equiv of $M(NMe_2)_4$ (M = Zr, Hf) in C_6D_6 resulted in formation of 2 equiv of $HNMe_2$ and the colorless bis(amido) complexes (eq 7). No intermediate species were observed.

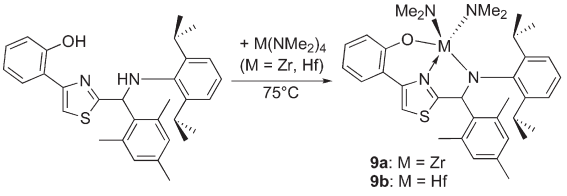

(7)

The structure of **9b** was determined by X-ray diffraction and is shown in Figure 10. Unlike the tris(amido) complex (**4**) and

dx.doi.org/10.1021/cs200180x |ACS Catal. 2011, 1, 887–900

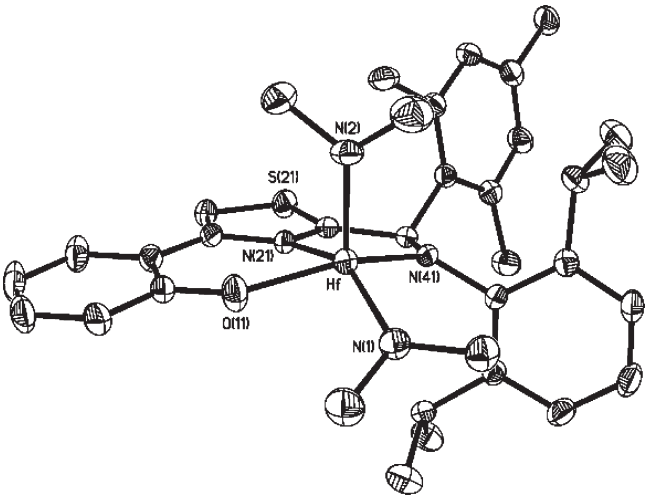

Figure 10. Molecular structure of **9b**. (Hydrogen atoms omitted for clarity) (Selected Bond Lengths (Å) Hf−N(21) 2.33, Hf−N(41) 2.14, Hf−N(2) 2.03, Hf−N(1) 2.03, Hf−O 1.99. Selected Bond Angles (deg) N(2)−Hf−N(41) 106.0, N(2)−Hf−N(21) 105.3, N(2)−Hf−N(1) 107.3, N(21)−Hf−N(1) 146.9).

trimethyl complex (**5**) and the orthometalated pyridyl amines, which all have trigonal bipyramidal geometries,[33] **9b** has a square pyramidal geometry.

For comparison purposes, the analogous pyridyl-amido complex with a phenoxide substituent (**10**) at R3 was prepared and screened under identical conditions.

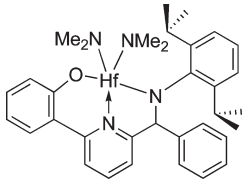

10

Complexes **8a**−**b**, **9a-b**, and **10** were activated and screened in the PPR, and the results are shown in Table 3. All five complexes produced highly crystalline polypropylene, albeit with low activity. For **8a**, the polymer melting point (entry 1, 152 °C) was the same as observed when complex **7** was tested, suggesting that a common intermediate is the active species in the polymerization. For the Hf complex **8b**, the activity and polymer melting point were similar to the Zr complex, **8a**, but the resulting polymer had lower molecular weight (200k vs 670k). The complexes with R3 = Mes (**9a**−**b**) had activity similar to **8a**−**b**, and the resulting polypropylene had higher FT-IR indices and higher melting points, but had lower molecular weight for both Zr and Hf. These trends are consistent with other thiazole-amines and pyridyl-amines, which show higher stereoselectivity and lower M_w as the steric bulk of R3 is increased.

The phenoxide pyridyl-amido complex **10** has very similar performance to **8a**−**b** and **9a**−**b**. In comparison, related pyrrole pyridyl-amido complexes, which lack a bulky substituent at R3 and a chiral center, have low activity and produce polypropylene with a lower degree of stereospecificity.[54,55]

The data suggest that the phenoxide species is a precatalyst in the polymerization. In comparing the two types of thiazole-amido catalysts with the pyridyl-amido catalysts, the following trends are apparent. The thiazole-amido phenoxide and pyridyl-amido phenoxide catalysts which contain a M−O bond, a six-member metallacycle, and a five- or six-member heterocycle, exhibit high stereoselectivity but low activity. The thiazole-amido

Table 3. Polymerization of Propylene by Complexes 8a−b, 9a−b, and 10[a]

entry	complex	alkylator	activity[b]	M_w(k)	FT-IR index	Mp (°C)
1	**8a**	5 DIBAL	27	670	0.88	152
2	**8b**	5 DIBAL	30	200	0.91	158
3	**9a**	10 DIBAL	48	186	0.95	151
4	**9b**	10 DIBAL	27	90	0.97	156, 162
5	**10**	10 DIBAL	44	380	0.9	147

[a] Toluene, 100 psi C_3H_6, 75 °C, ABF20 activation. [b] mg/(μmol catalyst* min).

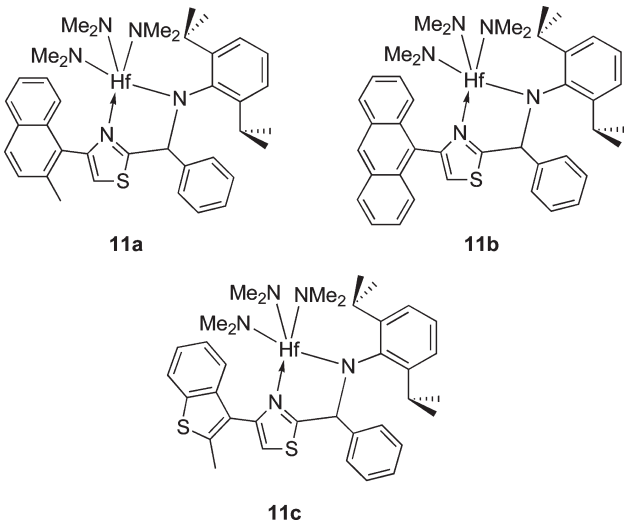

11a **11b**

11c

Figure 11. Thiazole-amido complexes to test 6-member metallacycle hypothesis.

Table 4. Polymerization of Propylene by Complexes 11a−c[a]

entry	complex	activity[b]	M_w(k)	FT-IR index	Mp (°C)
1	**11a**	20	50	0.37	n.d.
2	**11b**	41	220[c]	0.5	127[d]
3	**11c**	830	450	0.86	132

[a] Toluene, 100 psi C_3H_6, 110 °C, 15 TMA/ABF20 activation. [b] mg/(μmol catalyst*min). [c] Bimodal, M_w/M_n = 13.2. [d] Biphasic polymer.

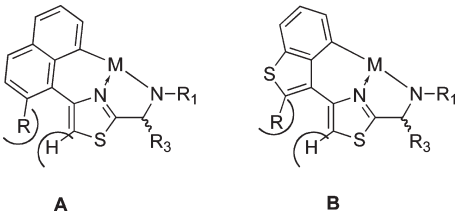

A **B**

Figure 12. Proposed steric interactions upon formation of 6-member metallacycle.

dx.doi.org/10.1021/cs200180x |*ACS Catal.* 2011, 1, 887–900

Table 5. Polymerization Data for 6-Member Ring SAR Study[a]

entry	ligand	in situ/isolated?[b]	activation conditions	activity[c]	M_w(k)	T_m (°C)
1	**11c**	isolated	15 TMA/ABF20	830	450	132
2	**12a**	in situ ($HfBn_3^+$)	5 PMAO/ABF20	370	690	128
3	**12b**	in situ ($HfBn_3^+$)	5 PMAO/ABF20	720	134	137
4	**12c**	in situ ($HfBn_3^+$)	5 PMAO/ABF20	540	474	141
5	**12d**	in situ ($HfBn_3^+$)	5PMAO/ABF20	840	309	145
6	**12e**	isolated	15TMA/ABF20	1910	309	121, 128
7	**13a**	isolated	15TMA/TBF20	1400	110	135, 144
8	**13b**	in situ ($Hf(NMe_2)_4$)	15TMA/ABF20	3300	90	123
9	**13c**	isolated	15TMA/ABF20	4500	80	144
10	**1f**	isolated	5 PMAO/ABF20	700	120	146
11	**14**	isolated	15TMA/ABF20	1100	250	125

[a] 110°C, toluene, 100 psi C_3H_6. [b] In situ complexation for 30 min at 75 °C. [c] mg/(μmol catalyst*min).

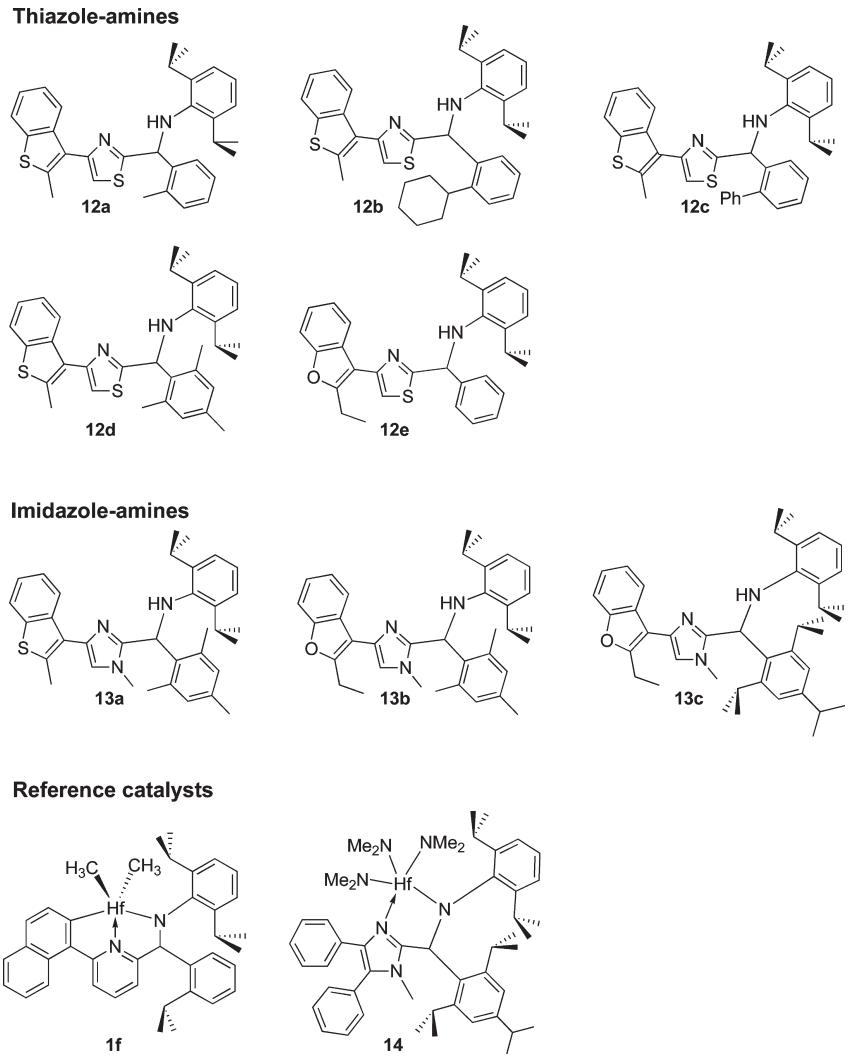

Figure 13. Thiazole-and imidazole amine ligands tested in the 6-member ring SAR study.

complexes, which contain a M−C bond, a five-member metallacycle, and a five-member heterocycle, exhibit high activity and lower stereoselectivity, and the pyridyl-amido complexes, which contain a M−C bond, a five-member metallacycle, and a six-member heterocycle, exhibit high activity and stereoselectivity. We hypothesized that the expanded metallacycle ring is responsible for higher stereoinduction and the metal−carbon bond is responsible for high activity, either as a spectator ligand or when involved in insertion of monomer into the M-aryl bond, as shown in Scheme 1.

dx.doi.org/10.1021/cs200180x |ACS Catal. 2011, 1, 887–900

At the time that this work was taking place, the observation of olefin insertion into the pyridyl-amido Hf−Ar bond had not yet been reported. However, if the olefin insertion is also occurring in these systems, it is consistent with the observation that the phenoxide complexes have lower activity than the analogous carbon metallacycles, since olefin insertion into a Hf−O bond is expected to be strongly disfavored. This observation is consistent with the hypothesis that the expanded ring is advantageous to stereospecificity, but the Hf−O bond results in low activity.

Catalyst Optimization. To test this hypothesis, thiazole-amines containing R2 substituents which would be likely to form 6-member metallacyles upon orthometalation were designed. Three R2 substituents were selected which could potentially form 6-membered rings via orthometalation without any competing formation of five-member metallacycles (Figure 11). The Hf complexes **11a**−**c** were activated and screened in the PPR at 110 °C (Table 4).

Complexes **11a** and **11b** had very low activity, and the resulting polypropylene was not highly isotactic. The polymer produced by **11b** had a bimodal M_w distribution (M_w/M_n = 13.2) and was visibly biphasic. A weak melting point was observed at 127 °C, suggesting that there may be more than one active species in the polymerization, and a small amount of orthometalated product may be formed. In contrast to **11a**−**b**, **11c** showed high activity, yielding polymer with high M_w and higher crystallinity. At 75 °C **11c** exhibited activities ranging from 2000 to 2700 mg/(μmol catalyst min) and produced polypropylene with T_m = 130−132 °C.

If orthometalation is occurring in the activated products of **11a**−**b**, there may be unfavorable steric interactions between H_a on the thiazole ring and the methyl or the other side of the anthracenyl ring (Figure 12, A). These interactions are predicted to be somewhat lessened in **11c** (Figure 12, B) because of the five membered benzothiophene ring, and orthometalation may be more likely to occur. This hypothesis is supported by the low activity of complexes **11a**−**b** compared to **11c**, as well as the observation that **11c** readily undergoes orthometalation at 70 °C, whereas **11a**−**b** do not.

A structure−activity relationship (SAR) study (Table 5) was then conducted to further optimize the Hf heteroaryl-amido catalysts. In addition to thiazole-amines, a variety of imidazole-amines were tested.[56] Selected examples are shown in Figure 13; a more comprehensive set of ligands and polymerization data is provided in the Supporting Information. At R2, 2-methylbenzothiophene (2MeBZT) and 2-ethylbenzofuran (2EtBZF) derivatives were tested, and R3 included a variety of aryl and substituted aryl rings. Data for thiazole- and imidazole-amido complexes containing napthyl- and phenyl substituents, respectively, at R2, are included for comparison purposes, as is data for an optimized pyridyl-amido complex, [DIP,Nap, 2-*i*PrPh]$HfMe_2$ (**1f**). The ligands were complexed to $Hf(NMe_2)_4$ in situ or the isolated Hf tris(dimethylamido) complexes were screened at 110 °C in the PPR.

Several trends were noted. The heterocycle dramatically influences the catalyst performance. When R1, R2, and R3 are held constant and the heteroaryl-amine is varied, the thiazole-amido catalysts yield polymer with higher molecular weight and a higher degree of isotacticity, while the imidazole-amido catalysts typically show higher activity (entry 5 vs 7).

When R1, R2, and the heterocycle are held constant, increased steric bulk at R3 results in increased stereoinduction

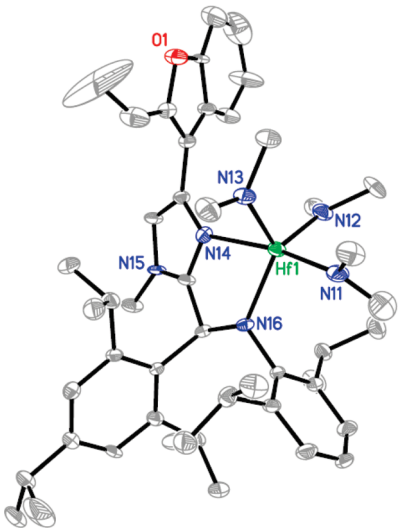

Figure 14. Molecular structure of **15** (hydrogen atoms omitted for clarity). (Selected Bond Lengths (Å) Hf−N(16) 2.17, Hf−N(14) 2.44, Hf−N(11) 2.06, Hf−N(12) 2.05, Hf−N(13) 2.05. Selected Bond Angles (deg) N(12)−Hf−N(11) 97.7, N(12−Hf−N(13) 111.8, N(12)−Hf−N(14) 88.3, N(12)−Hf−N(16) 117.2, N(11)−Hf−N(13) 92.2, N(11)−Hf−N(14) 171.6, N(11)−Hf−N(16) 100.3, N(13)−Hf−N(14) 90.9, N(13)−Hf−N(16) 126.9, N(14)−Hf−N(16) 71.7).

for both the thiazole- and imidazole-amido catalysts. For instance, in entries 1−5 in the table, the polymer T_m increases 13 °C as R3 is varied from phenyl to mesityl. The substituent at R2 has a dramatic influence on the catalyst performance. Both 2-MeBZT and 2-EtBZF proved to be suitable substituents, yielding catalysts with high activity and steroinduction. When 2-MeBZT and 2-EtBZF are compared, higher stereoinduction is observed for 2-MeBZT. This is observed for both thiazoles (entry 1 vs 6) and imidazoles (entry 7 vs 8). However, higher activity is observed for the 2-EtBZF derivatives, especially for the imidazole-amines. Because of the electrophilic metal center, ligand substituents containing potentially coordinating hereroatoms have not been widely explored in Group 4 olefin polymerization catalysts; however, these results suggest that certain catalysts may tolerate functionality at peripheral sites.

The dramatic effect of the 2-EtBZF substitution at R2 is apparent from the comparison of the performance of the Hf complex of **13c** (entry 9) with the first-generation imidazole-amido complex, **14** (entry 11), which has a phenyl substituent at R2. For **13c**/**Hf**, activity is 4 times higher and the resulting polymer has a T_m which is 19 °C higher.

Since the combination of **13c**/Hf showed superior activity and stereocontrol, the characterization and reactivity of isolated Hf tris(amide) and trimethyl complexes of **13c** was studied. Complex **15** is prepared in 70% yield from the reaction of **13e** with $Hf(NMe_2)_4$ (eq 8). The analogous trimethyl complex can be prepared by reaction of **15** with $AlMe_3$ or via reaction with excess Me_3SiCl followed by alkylation with MeMgBr.[57] **15** was characterized by X-ray diffraction, and its molecular structure is shown in Figure 14. Like the thiazole-amido complexes **4** and **5**, **15** has a distorted trigonal bipyramidal geometry. The Hf−N(imidazole) bond length (2.44 Å) is slightly shorter than the Hf−N(thiazole) length in **4** (2.49 Å), consistent with

dx.doi.org/10.1021/cs200180x |*ACS Catal.* 2011, 1, 887–900

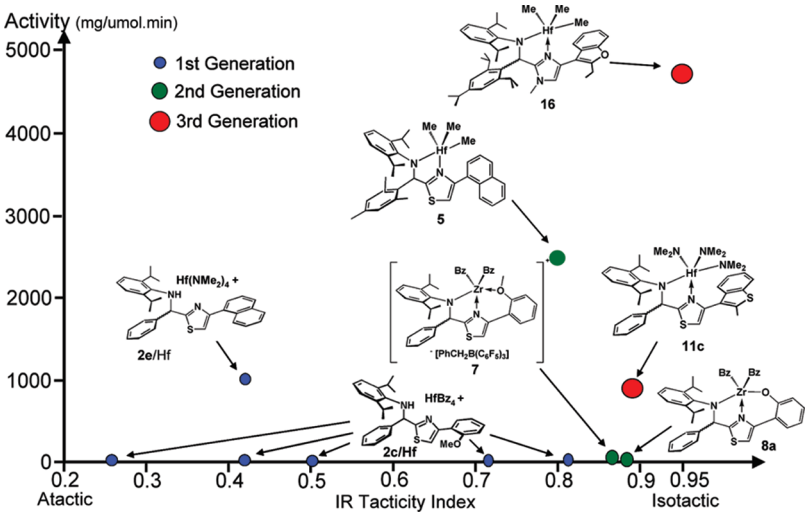

Figure 15. Comparison of performance of first, second, and third generation heteroaryl-amido Hf catalysts.

higher basicity of the imidazole imine relative to the thiazole imine.

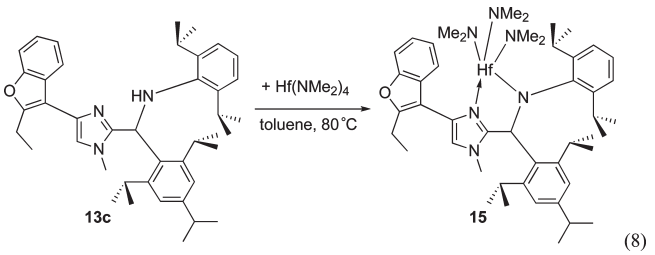

(8)

Of all the catalysts screened, **15** exhibits the best combination of activity and stereospecificity. Comparing **15** to the benchmark pyridyl-amido complex **1f**, the activity of **15** is >6 times higher, and polymer molecular weight and T_m are similar. At 130 °C, the activity difference is even more pronounced (**15**: A = 1300; **1f**: A = 80), and polymer properties are similar. Thus, the optimization of the heteroaryl-amine catalysts has resulted in a substantial improvement in the catalyst performance at high temperature.

The evolution of the Hf heteroaryl-amido catalysts is shown in Figure 15.[58] As can be seen, the performance of this class of catalysts improved dramatically with each successive generation and surpasses that of the pyridyl-amido systems.

CONCLUSIONS

In summary, the zirconium and hafnium heteroaryl-amido complexes have proven to be excellent catalysts for the stereospecific polymerization of propylene and have several advantages over the related pyridyl-amido systems, namely, higher activity and, in some cases, higher molecular weight. The heteroaryl-amine ligand class was optimized through a synergistic combination of high-throughput experimentation and traditional organometallic chemistry. Although some of the initial thiazole-amines screened showed high activity for propylene polymerization when complexed to Zr or Hf and produced polypropylene with very high molecular weight, the resulting polypropylene from most of the catalyst systems was not highly isotactic. However, the use of a broad range of activation conditions in the primary screen led to the serendipitous discovery of high stereospecificity when **2c** was screened in the presence of BF_{15} and AlR_3. The resulting discovery that demethylation was occurring, resulting in a phenoxide complex, suggested that structures with expanded metallacycles might be advantageous in terms of stereospecificity. The resulting SAR studies led to a number of highly optimized catalysts with bulky aryl substituents at R1 and R3 and very nontraditional substituents at R2. This case study nicely illustrates the power of high throughput screening methods when combined strategically with traditional organometallic chemistry.

EXPERIMENTAL SECTION

Unless otherwise noted, all manipulations were conducted under an atmosphere of dry, deoxygenated argon in a Vacuum Atmospheres or MBraun glovebox. $HfCl_4$, MBn_4 (M = Hf, Zr), and $M(NMe_2)_4$ (M = Zr, Hf) were purchased from Strem Chemicals. $[MBn_3][BnB(C_6F_5)_3]$ (M = Hf, Zr) was synthesized as described in the literature.[51] $[Ph_3C]^+[B(C_6F_5)_4]^-$ (TBF_{20}) and $[PhNMe_2H]^+[B(C_6F_5)_4]^-$ (ABF_{20}) were purchased from Single-Site Catalysts, LLC. $B(C_6F_5)_3$ (BF_{15}) was purchased from Boulder Scientific. Diethyl ether, tetrahydrofuran, pentane, and toluene were sparged with nitrogen and passed though columns of activated Al_2O_3 and CU-0226S (Engelhart; a commercially available oxygen scavenger).[59] Anhydrous benzene-d_6 and toluene-d_8 were purchased from Cambridge Isotopes, degassed, and stored over 4 Å molecular sieves. All other reagents were purchased from Aldrich in the highest available purity and used without further purification. Synthetic information for the heteroaryl-amine ligands can be found in the patent literature.[49]

NMR spectra were recorded on a Bruker 300 MHz spectrometer. ^{1}H chemical shifts were referenced relative to residual protio solvent peaks. Because of the large number of aromatic substituents and the complexity of the spectra in the 6.8−7.5 ppm region, the peaks corresponding to the hydrogens on the aromatic rings are generally not assigned and are denoted as "Ar" in the lists of NMR data.

Nomenclature. For simplicity, the complexes will be abbreviated as follows: 2-((R1N (R3CH))-(5-R2)-heteroaryl)MX_n =

dx.doi.org/10.1021/cs200180x |ACS Catal. 2011, 1, 887–900

Heteroaryl-amido [R1, R2, R3]MX_n. A schematic is shown below.

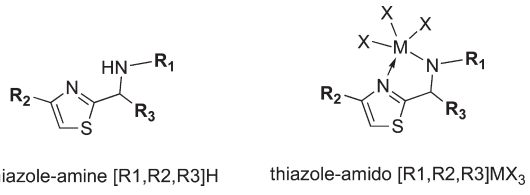

thiazole-amine [R1,R2,R3]H thiazole-amido [R1,R2,R3]MX_3

Thiazole-amido [DIP, Nap, Mes]Hf(NMe_2)$_3$ (4). Solid **3** (52 mg, 0.1 mmol) and Hf(NMe_2)$_4$ (46 mg, 0.13 mmol) were combined, and 2 mL of toluene was added. The mixture was heated to 110 °C for 2 d with occasional venting. Solvent was removed, and the resulting solid was recrystallized from pentane at −35 °C. The identity of the complex was confirmed by ^{1}H NMR and X-ray structure determination. (64 mg, 77%) ^{1}H NMR (δ, C_6D_6) 7.0−7.4 (m, 10, Ar), 6.74 (s, 1, Mes Ar), 6.58 (s, 1, thiazole SC-*H*), 6.50 (s, 1, Mes Ar), 6.47 (s, 1, C*H*Mes), 3.76 (sept., 1, C*H*(CH_3)$_2$), 3.43 (sept., 1, C*H*(CH_3)$_2$), 2.90 (br s, 6, NMe_2), 2.64 (br s, 6, NMe_2), 2.48 (br s, 6, NMe_2), 2.31 (s, 3, $MesCH_{3(a)}$), 2.07 (s, 3, $MesCH_{3(b)}$), 1.84 (s, 3, $MesCH_{3(c)}$), 1.59 (d, 3, CH(C*H*$_3$)$_2$), 1.52 (d, 3, CH(C*H*$_3$)$_2$), 1.23 (d, 3, CH(C*H*$_3$)$_2$), 0.37 (d, 3, CH(C*H*$_3$)$_2$).

Thiazole-amido [DIP, Nap, Mes]Hf(CH_3)$_3$ (5). **4** (45 mg, 0.054 mmol) was dissolved in 7 mL of pentane. The mixture was cooled to −35 °C. Neat $AlMe_3$ (52 μL, 0.54 mmol) was added. A pale yellow oil precipitated which dissolved as the mixture was allowed to warm to room temperature. The mixture was stirred for 1 h and then solvent was removed. The resulting colorless solid was recrystallized from pentane at −35 °C (24 mg, 60%). The identity of the complex was confirmed by ^{1}H NMR and X-ray structure determination. ^{1}H NMR (δ, tol-d_8) 7.70 (m, 4, Ar), 7.0−7.4 (m, 6, Ar), 6.78 (s, 1, Mes Ar), 6.64 (s, 1, Mes Ar), 6.54 (s, 1, thiazole SC-*H*), 6.45 (s, 1, C*H*Mes), 3.76 (sept., 1, C*H*(CH_3)$_2$), 3.53 (sept., 1, C*H*(CH_3)$_2$), 2.38 (s, 3, $MesCH_{3(a)}$), 2.15 (s, 3, $MesCH_{3(b)}$), 1.86 (s, 3, $MesCH_{3(c)}$), 1.46 (d, 3, CH(C*H*$_3$)$_2$), 1.42 (d, 3, CH(C*H*$_3$)$_2$), 0.92 (d, 3, CH(C*H*$_3$)$_2$), 0.35 (d, 3, CH(C*H*$_3$)$_2$), 0.28 (s, 9, Hf(C*H*$_3$)$_3$).

Thiazole-amido [DIP, 2-OMePh, Ph]Zr(CH_2Ph)$_2$ (6). Solid **2c** (48 mg, 0.11 mmol) and Zr(CH_2Ph)$_4$ (50 mg, 0.11 mmol) were combined, and 2 mL of benzene was added. The mixture was heated to 75 °C for 4 h. Solvent was removed, and the resulting solid was dissolved in hot hexane and filtered. The volume was reduced to 1 mL and cooled to −35 °C. A yellow precipitate formed which was collected and dried. (52 mg, 58%) ^{1}H NMR (δ, C_6D_6) 7.94 (d, 2, Ar), 6.3−7.3 (m, 19, Ar+ thiazole), 6.01 (s, 1, C*H*Ph), 3.35 (s, 3, OMe) 3.32 (overlapping sept., 2, C*H*(CH_3)$_2$), 2.80 (d, 1, C*H*$_2$Ph), 2.50 (s, 2, C*H*$_2$Ph), 2.34 (d, 1, C*H*$_2$Ph), 1.37 (d, 3, CH(C*H*$_3$)$_2$), 1.28 (d, 3, CH(C*H*$_3$)$_2$), 1.18 (d, 3, CH(C*H*$_3$)$_2$), 0.04 (d, 3, CH(C*H*$_3$)$_2$).

Thiazole-amido [DIP, 2-OMePh, Ph]Zr(CH_2Ph)$_2^+$[$PhCH_2B(C_6F_5)_3$]$^-$ (7). Solid **2c** (27 mg, 0.06 mmol), Zr(CH_2Ph)$_4$ (28 mg, 0.06 mmol), and B(C_6F_5)$_3$ (32 mg, 0.06 mmol) were combined, and 2 mL of toluene was added. The mixture was stirred at room temperature for 30 min, yielding an orange solution. Three milliliters of pentane was added, and the total volume was reduced to 2 mL. The mixture was cooled to −35 °C. A yellow-orange oil precipitated. The oil was collected, washed with pentane, and dried, yielding an orange-yellow solid. (54 mg, 68%) 5.8−7.5 (m, 29, Ar+ thiazole + C*H*Ph), 3.78 (sept., 1, C*H*(CH_3)$_2$), 3.39 (s, 3, OMe), 3.36 (br s, 2, BC*H*$_2$Ph), 3.20 (sept., 1, C*H*(CH_3)$_2$), 2.92 (sept., 1, C*H*(CH_3)$_2$), 2.60 (d, 1, C*H*$_2$Ph), 2.43 (s, 2, C*H*$_2$Ph), 1.57 (overlapping d, 2, C*H*$_2$Ph), 1.85 (d, 1, C*H*$_2$Ph), 1.42 (d, 3, CH(C*H*$_3$)$_2$), 1.18 (d, 3, CH(C*H*$_3$)$_2$), 1.13 (d, 3, CH(C*H*$_3$)$_2$), 0.07 (d, 3, CH(C*H*$_3$)$_2$).

Thiazole-amido [DIP, 2-OPh, Ph]Zr(CH_2Ph)$_2$ (8a). Solid [DIP, 2-OHPh, Ph]H (75 mg, 0.17 mmol) was dissolved in 2 mL of benzene. Zr(CH_2Ph)$_4$ (81 mg, 0.18 mmol) was dissolved in 2 mL of benzene, and this solution was added to the ligand solution with stirring. The mixture was stirred at room temperature for 1 h, and then solvent was removed. The resulting solid was recrystallized from pentane at −35C. ^{1}H NMR (δ, C_6D_6) 6.5−7.5 (m, 19, Ar+ thiazole), 5.89 (s, 1, C*H*Ph), 3.58 (sept., 1, C*H*(CH_3)$_2$), 3.10 (sept., 1, C*H*(CH_3)$_2$), 2.90 (d, 1, C*H*$_2$Ph), 1.8−2.1 (overlapping d, 3, C*H*$_2$Ph), 1.45 (d, 3, CH-(C*H*$_3$)$_2$), 1.33 (d, 3, CH(C*H*$_3$)$_2$), 1.18 (d, 3, CH(C*H*$_3$)$_2$), 0.10 (d, 3, CH(C*H*$_3$)$_2$).

Thiazole-amido [DIP, 2-OPh, Ph]Hf(CH_2Ph)$_2$ (8b). Solid thiazole-amine[DIP, 2-OHPh, Ph]H (50 mg, 0.11 mmol) was dissolved in 2 mL of benzene. Hf(CH_2Ph)$_4$ (68 mg, 0.13 mmol) was dissolved in 2 mL of benzene, and this solution was added to the ligand solution with stirring. The mixture was stirred at room temperature for 2 h, and then solvent was removed. The resulting off-white solid was precipitated from pentane and dried. ^{1}H NMR was consistent with the proposed structure.

Thiazole-amido [DIP, 2-OPh, Mes]Zr(NMe_2)$_2$ (9a). Solid thiazole-amine [DIP, 2-OHPh, Mes]H (20 mg, 0.04 mmol) was dissolved in 1 mL of benzene. Zr(NMe_2)$_4$ (12 mg, 0.04 mmol) was dissolved in 1 mL of benzene, and this solution was added to the ligand solution. The mixture was heated to 65 °C for 1 h, at which time ^{1}H NMR revealed that the reaction was complete. Solvent was removed, and the resulting off-white solid was recrystallized from pentane. (14 mg, 53%) ^{1}H NMR (δ, C_6D_6) 6.75−7.4 (m, 7, Ar), 6.73 (s, 1, Mes Ar), 6.55 (s, 1, Mes Ar), 6.52 (s, 1, thiazole SC-*H*), 6.20 (s, 1, C*H*Mes), 3.69 (sept., 1, C*H*(CH_3)$_2$), 3.09 (sept., 1, C*H*(CH_3)$_2$), 2.95 (s, 6, N*Me*$_2$), 2.79 (s, 6, N*Me*$_2$), 2.20 (s, 3, $MesCH_{3(a)}$), 2.06 (s, 3, $MesCH_{3(b)}$), 1.73 (s, 3, $MesCH_{3(c)}$), 1.34 (d, 3, CH(C*H*$_3$)$_2$), 1.27 (d, 3, CH(C*H*$_3$)$_2$), 1.14 (d, 3, CH(C*H*$_3$)$_2$), 0.39 (d, 3, CH(C*H*$_3$)$_2$).

Thiazole-amido [DIP, 2-OPh, Mes]Hf(NMe_2)$_2$ (9b). Solid thiazole-amine [DIP, 2-OHPh, Mes]H (21 mg, 0.04 mmol) was dissolved in 1 mL of benzene. Hf(NMe_2)$_4$ (17 mg, 0.05 mmol) was dissolved in 1 mL of benzene, and this solution was added to the ligand solution. The mixture was heated to 65 °C for 22 h, at which time ^{1}H NMR revealed that the reaction was complete. Solvent was removed, and the resulting off-white solid was recrystallized from pentane. The structure of the complex was confirmed by ^{1}H NMR and X-ray crystallography. ^{1}H NMR (δ, C_6D_6) 6.7−7.4 (m, 7, Ar), 6.71 (s, 1, Mes Ar), 6.53 (s, 1, Mes Ar), 6.51 (s, 1, thiazole SC-*H*), 6.34 (s, 1, C*H*Mes), 3.69 (sept., 1, C*H*(CH_3)$_2$), 3.15 (sept., 1, C*H*(CH_3)$_2$), 2.98 (s, 6, N*Me*$_2$), 2.85 (s, 6, N*Me*$_2$), 2.19 (s, 3, $MesCH_{3(a)}$), 2.10 (s, 3, $MesCH_{3(b)}$), 1.72 (s, 3, $MesCH_{3(c)}$), 1.33 (d, 3, CH(C*H*$_3$)$_2$), 1.27 (d, 3, CH(C*H*$_3$)$_2$), 1.19 (d, 3, CH(C*H*$_3$)$_2$), 0.38 (d, 3, CH(C*H*$_3$)$_2$).

Thiazole-amido [DIP, Anth, Ph]Hf(NMe_2)$_3$ (11b). Solid [DIP,Anth,Ph]H (199 mg, 0.38 mmol) and Hf(NMe_2)$_4$ (160 mg, 0.45 mmol) were combined, and 4 mL of benzene was added. The mixture was heated to 70 °C for 1 h. Solvent was removed, and the resulting yellow oil was recrystallized from pentane at −35 °C. (164 mg, 52%) ^{1}H NMR (δ, C_6D_6) 8.35 (d, 2, Ar), 7.40 (d, 2, Ar), 6.8−7.3 (m, 14, Ar + thiazole), 6.05 (s, 1, C*H*Ph), 3.67

dx.doi.org/10.1021/cs200180x |*ACS Catal.* 2011, 1, 887–900

(sept., 1, C*H*(CH_3)$_2$), 3.24 (overlapping sept + s, 7, C*H*(CH_3)$_2$ + N(CH_3)$_2$), 2.88 (s, 6, N*Me*$_2$), 2.84 (s, 6, N*Me*$_2$), 1.54 (d, 3, CH(CH_3)$_2$), 1.48 (d, 3, CH(CH_3)$_2$), 1.37 (d, 3, CH(CH_3)$_2$), 0.32 (d, 3, CH(CH_3)$_2$).

Thiazole-amido [DIP, 2MeBZT, Ph]Hf(NMe$_2$)$_3$ (11c). Solid thiazole-amine [DIP,2MeBZT,Ph]H (36 mg, 0.073 mmol) and Hf(NMe$_2$)$_4$ (28 mg, 0.08 mmol) were combined, and 2 mL of benzene was added. The mixture was stirred for 1 h at room temperature. Solvent was removed, and the resulting solid was recrystallized from pentane at −35 °C. (37 mg, 60%) ^{1}H NMR (δ, C_6D_6) 6.9−7.5 (m, 12, Ar), 6.31 (s, 1, thiazole SC-*H*), 6.10 (s, 1, C*H*Ph), 3.69 (sept., 1, C*H*(CH_3)$_2$), 3.33 (sept., 1, C*H*(CH_3)$_2$), 2.7 (br s, 18, N*Me*$_2$), 2.32 (s, 3, benzothiophene CH_3), 1.62 (d, 3, CH(CH_3)$_2$), 1.48 (d, 3, CH(CH_3)$_2$), 1.27 (d, 3, CH(CH_3)$_2$), 0.24 (d, 3, CH(CH_3)$_2$)

Imidazole-amido [DIP, Ph, TRIP, Ph, NMe]Hf(NMe$_2$)$_3$ (14). Solid imidazole-amine [DIP,Ph,TRIP,Ph,NMe]H (182 mg, 0.29 mmol) and Hf(NMe$_2$)$_4$ (119 mg, 0.34 mmol) were combined, and 5 mL of toluene was added. The mixture was heated to 50 °C for 3 h. Solvent was removed, and the resulting colorless solid was recrystallized from pentane at −35 °C. (234 mg, 87%) ^{1}H NMR (δ, C_6D_6) 7.62 (m, 2, Ar), 6.85−7.3 (m, 13, Ar), 6.35 (s, 1, C*H*TRIP), 3.91 (sept., 1, C*H*(CH_3)$_2$), 3.74 (sept., 1, C*H*(CH_3)$_2$), 3.61 (sept., 1, C*H*(CH_3)$_2$), 3.13 (s, 6, NMe$_2$), 2.91 (s, 6, NMe$_2$), 2.82 (s, 6, NMe$_2$), 2.73 (sept., 1, C*H*(CH_3)$_2$), 2.35 (s, 3, imidazole NCH_3), 1.65 (d, 3, CH(CH_3)$_2$), 1.58 (d, 3, CH(CH_3)$_2$), 1.42 (d, 3, CH(CH_3)$_2$), 1.31 (d, 3, CH(CH_3)$_2$), 1.19 (overlapping d, 6, CH(CH_3)$_2$), 1.06 (d, 3, CH(CH_3)$_2$), 0.78 (d, 3, CH(CH_3)$_2$), 0.51 (d, 3, CH(CH_3)$_2$), 0.24 (d, 3, CH(CH_3)$_2$).

Imidazole-amido [DIP, 2-EtBZF, TRIP, H, NMe]Hf(NMe$_2$)$_3$ (15). Solid Hf(NMe$_2$)$_4$ (71 mg, 0.20 mmol) and **13e** (103 mg, 0.17 mmol) were combined and dissolved in 5 mL of toluene. The mixture was heated to 80 °C overnight. ^{1}H NMR of an aliquot revealed that the reaction was complete. Solvent was removed, and the resulting glassy yellow solid was dissolved in 5 mL of pentane, filtered, and solvent was removed, yielding a pale yellow solid containing traces of residual Hf(NMe$_2$)$_4$. The material was recrystallized from pentane at −35 °C (110 mg, 70%). The solid state structure was determined by X-ray crystallography. ^{1}H NMR (δ, C_6D_6) 7.58 (d, 1, Ar), 7.41 (d, 1, Ar), 6.9−7.2 (m, 7, Ar), 6.17 (s, 1 imidazole C*H*), 5.90 (s, 1, C*H*TRIP), 3.84 (sept., 1, C*H*(CH_3)$_2$), 3.62 (sept., 1, C*H*(CH_3)$_2$), 3.56 (sept., 1, C*H*(CH_3)$_2$), 3.02 (sept., 1, C*H*(CH_3)$_2$), 2.92 (s, 6, NMe$_2$), 2.87 (s, 6, NMe$_2$), 2.69 (sept., 1, C*H*(CH_3)$_2$), 2.64 (s, 6, NMe$_2$), 2.73 (sept., 1, C*H*(CH_3)$_2$), 2.30 (s, 3, imidazole NCH_3), 1.55 (d, 6, CH(CH_3)$_2$), 1.31 (p, 6, overlapping CH(CH_3)$_2$ and CH_2CH_3), 1.19 (overlapping d, 6, CH(CH_3)$_2$), 1.06 (d, 3, CH(CH_3)$_2$), 0.71 (d, 3, CH(CH_3)$_2$), 0.52 (d, 3, CH(CH_3)$_2$), 0.27 (d, 3, CH(CH_3)$_2$). Note: The CH_2CH_3 peaks from the 2-Ethylbenzofuran are obscured by the amido peaks.

■ ASSOCIATED CONTENT

Supporting Information. Experimental description of the high-throughput polymerization workflows, polymerization data from additional thiazole- and imidazole-amine catalysts, synthesis and charactization of the trimethyl analogue of **15**, and crystallographic information files (CIF) for complexes **7**, **5**, **9b**, and **15**. This material is available free of charge via the Internet at http://pubs.acs.org.

■ AUTHOR INFORMATION

Corresponding Author

*E-mail: lapointe@cornell.edu. Phone: (607) 255-5401.

Present Addresses

[†]Department of Chemistry and Chemical Biology, Baker Laboratory, Cornell University, Ithaca, NY 14853.
[‡]Rennovia, Inc., 1080 Hamilton Avenue, Menlo Park, CA 94025.
[§]Freeslate, Inc., 415 Oakmead Parkway, Sunnyvale, CA 94085.
[∥]Department of Chemistry, University of California, Berkeley, California 94720.

■ ACKNOWLEDGMENT

We thank Drs. Lily Ackerman, Xiaohong Bei, Tom Boussie, Vince Murphy, and Howard Turner for helpful discussions, Ms. Jessica Zhang for ligand synthesis, Mr. Jeff Harris and Peter Huefner for polymer analysis, Dr. Guang Zhu for assistance with the X-ray data, and Ms. Vivian Luo for ligand archiving.

■ REFERENCES

(1) Brintzinger, H. H.; Fischer, D.; Mulhaupt, R.; Rieger, B.; Waymouth, R. M. *Angew Chem., Int. Ed. Engl.* **1995**, *34*, 1143.
(2) Resconi, L.; Cavallo, L.; Fait, A.; Piemontesi, F. *Chem. Rev.* **2000**, *100*, 1253.
(3) Chen, E. X.-Y.; Marks, T. J. *Chem. Rev.* **2000**, *100*, 1391.
(4) Jordan, R. F.; Bajgur, C. S.; Willett, R.; Scott, B. *J. Am. Chem. Soc.* **1986**, *108*, 7410.
(5) Hlatky, G. G.; Turner, H. W.; Eckman, R. R. *J. Am. Chem. Soc.* **1989**, *111*, 2728.
(6) Jordan, R. F. *Adv. Organomet. Chem.* **1991**, *32*, 325.
(7) Christianson, M. D.; Tan, E. H. P.; Landis, C. R. *J. Am. Chem. Soc.* **2010**, *132*, 11461.
(8) Fu, G. C. *Acc. Chem. Res.* **2008**, *41*, 1555.
(9) Hartwig, J. F. *Acc. Chem. Res.* **2008**, *41*, 1534.
(10) Hartwig, J. F. *Acc. Chem. Res.* **1998**, *31*, 852.
(11) For a review of catalyst influence on polymer microstructure, see: Coates, G. W. *Chem. Rev.* **2000**, *100*, 1223, and references therein.
(12) Wasilke, J.-C.; Obrey, S. J.; Baker, R. T.; Bazan, G. C. *Chem. Rev.* **2005**, *105*, 1001.
(13) Komon, Z. J. A.; Diamond, G. M.; Leclerc, M. K.; Murphy, V.; Okazaki, M.; Bazan, G. C. *J. Am. Chem. Soc.* **2002**, *124*, 15280.
(14) Boffa, L. S.; Novak, B. *Chem. Rev.* **2000**, *100*, 1479.
(15) Liang, L.-C.; Schrock, R. R.; Davis, W. M.; McConville, D. H. *J. Am. Chem. Soc.* **1999**, *121*, 5797.
(16) Scollard, J. D.; McConville, D. H. *J. Am. Chem. Soc.* **1996**, *118*, 10008.
(17) Chen, A.; Kopilov, J.; Goldberg, I.; Kol, M. *Organometallics* **2009**, *28*, 1391.
(18) Kirrilov, E.; Roisnel, T.; Razavi, A.; Carpentier, J.-F. *Organometallics* **2009**, *28*, 5036.
(19) Capacchinoe, C.; Proto, A.; Ebeling, H.; Mülhaupt, R.; Moller, K.; Spaniol, T. P.; Okuda, J. *J. Am. Chem. Soc.* **2003**, *125*, 4964.
(20) Gibson, V. C.; Spitzmesser, S. K. *Chem. Rev.* **2003**, *103*, 283.
(21) Britzovek, G. J. P.; Gibson, V. C.; Wass, D. F. *Angew. Chem., Int. Ed.* **1999**, *38*, 424.
(22) Hustad, P. D.; Tian, J.; Coates, G. W. *J. Am. Chem. Soc.* **2002**, *124*, 3614.
(23) Wei, J.; Zhang, W.; Sita, L. R. *Angew. Chem., Int. Ed.* **2010**, *49*, 1768.
(24) Golisz, S. R.; Bercaw, J. E. *Macromolecules* **2009**, *42*, 8741.
(25) Ittel, S. D.; Johnson, L. K.; Brookhart, M. S. *Chem. Rev.* **2000**, *100*, 1169.
(26) Small, B. L.; Bennett, A. M. A.; Brookhart, M. *J. Am. Chem. Soc.* **1998**, *120*, 4049.

(27) Johnson, L. K.; Killian, C. M.; Brookhart, M. *J. Am. Chem. Soc.* **1995**, *117*, 6414.
(28) Younkin, T. R.; Connor, E. F.; Henderson, J. I.; Friedrich, S. K.; Grubbs, R. H.; Bansleben, D. A. *Science* **2000**, *287*, 460.
(29) Azoulay, J. D.; Rojas, R. S.; Serrano, A. V.; Ohtaki, H.; Galland, G. D.; Wu, G.; Bazan, G. C. *Angew. Chem., Int. Ed.* **2009**, *48*, 1089.
(30) Boussie, T. R.; Diamond, G. M.; Goh, C.; Hall, K. A.; LaPointe, A. M.; Leclerc, M. K.; Lund, C.; Murphy, V.; Shoemaker, J. A. M.; Tracht, U.; Turner, H.; Uno, T.; Zhang, J.; Rosen, R. K.; Stevens, J. C. *J. Am. Chem. Soc.* **2003**, *125*, 4306.
(31) Murphy, V.; Bei, X.; Boussie, T. R.; Brummer, O.; Diamond, G. M.; Goh, C.; Hall, K. A.; LaPointe, A. M.; Leclerc, M. K.; Longmire, J. M.; Shoemaker, J. A. W.; Turner, H. W.; Weinberg, H. *Chem. Rec.* **2002**, *2*, 278.
(32) Jandeleit, B.; Schaefer, D. J.; Powers, T. S.; Turner, H. W.; Weinberg, W. H. *Angew. Chem., Int. Ed.* **1999**, *38*, 2494.
(33) Boussie, T. R.; Diamond, G. M.; Goh, C.; Hall, K. A.; LaPointe, A, M.; Leclerc, M.; Murphy, V.; Shoemaker, J. A. W.; Turner, H.; Rosen, R. K.; Stevens, J. C.; Alfano, F.; Busico, V.; Cipullo, R.; Talarico, G. *Angew. Chem., Int. Ed.* **2006**, *45*, 3278.
(34) Boussie, T. R.; Diamond, G. M. ; Goh, C., Hall, K. A. ; LaPointe, A. M. ; Leclerc, M. K.; Lund, C. ; Murphy, V. (Symyx Technologies, Inc.) U.S. Patent 7018949, 2006.
(35) Boussie, T. R.; Diamond, G. M.; Goh, C., Hall, K. A.; LaPointe, A. M.; Leclerc, M. K.; Lund, C.; Murphy, V. (Symyx Technologies, Inc.) U.S. Patent 6750345, 2004.
(36) Boussie, T. R.; Diamond, G. M.; Goh, C.; Hall, K. A.; LaPointe, A. M.; Leclerc, M. K.; Lund, C.; Murphy, V. (Symyx Technologies, Inc.) U.S. Patent 6713577, 2004.
(37) Arriola, D. J.; Bokota, M.; Timmers, F. J. (Dow Chemical Co.) PCT Int. App. Publ. No. WO 2004/026925 A1.
(38) Frazier, K. A.; Boone, H.; Vosejpka, P. C.; Stevens, J. C. (Dow Chemical Co.) U.S. Pat. Appl. Publ. No. US 2004/0220050 A1
(39) Stevens, J. C.; Vanderlende, D. D. (Dow Chemical Co.) PCT Int. App. Publ. No WO 2003/040201 A1.
(40) Tau, L.-M.; Cheung, Y. W.; Diehl, C. F.; Hazlitt, L. G. (Dow Chemical Co.) U.S. Pat. Appl. Publ. No. US2004/0087751 A1
(41) Arriola, D. J.; Carnahan, E. M.; Hustad, P. D.; Kuhlman, R. L.; Wenzel, T. T. *Science* **2006**, *312*, 714.
(42) Hustad, P. D.; Marchand, G. R.; Garcia-Meitin, E. I.; Roberts, P. L.; Weinhold, J. D. *Macromolecules* **2009**, *42*, 3788.
(43) Zuccaccia, C.; Macchioni, A.; Cipullo, R.; Talarico, G.; Alfano, F.; Boone, H. W.; Frazier, K. A.; Hustad, P. D.; Stevens, J. C.; Vosejpka, P. C.; Abboud, K. A. *J. Am. Chem. Soc.* **2008**, *130*, 10354.
(44) Zuccacia, C.; Busico, V.; Cipullo, R.; Talarico, G.; Froese, R. D. J.; Vosejpka, P. C.; Hustad, P. D.; Macchioni, A. *Organometallics* **2009**, *28*, 5445.
(45) Busico, V.; Cipullo, R.; Pellecchia, R.; Rongo, L.; Talarico, G.; Macchioni, A.; Zuccaccia, C.; Froese, R. D. J.; Hustad, P. D. *Macromolecules* **2009**, *41*, 4369.
(46) Froese, R. D.; Hustad, P. D.; Kuhlman, R. L.; Wenzel, T. J. *J. Am. Chem. Soc.* **2007**, *129*, 7831.
(47) Domski, G. J.; Lobkovsky, E. B.; Coates, G. W. *Macromolecules* **2007**, *40*, 3510.
(48) Domski, G. J.; Edson, J. B.; Kertesztes, I.; Lobkovsky, E. B.; Coates, G. W. *Chem. Commun.* **2008**, 6137.
(49) Diamond, G. M.; LaPointe, A. M.; Leclerc, M. K.; Longmire, J.; Nava-Salgado, V. ; Shoemaker, J. A. W.; Sun, P. (Symyx Technologies, Inc.) U.S. Patent 7256296, 2007.
(50) Diamond, G. M.; LaPointe, A. M.; Leclerc, M. K.; Longmire, J.; Nava-Salgado, V. ; Shoemaker, J. A. W.; Sun, P. (Symyx Technologies, Inc.) U.S. Patent 7387980, 2008.
(51) Pellecchia, C.; Grassi, A.; Zambelli, A. *Organometallics* **1994**, *13*, 298–302.
(52) Pellecchia, C.; Grassi, A.; Immirzi, A. *J. Am. Chem. Soc.* **1993**, *115*, 1160–1162.
(53) Siemeling, U. *Chem. Rev.* **2000**, *100*, 1495 and references therein.
(54) Pellecchia, C.; Grassi, A.; Zambelli, A. *Organometallics* **1994**, *13*, 298–302.
(55) Pellecchia, C.; Grassi, A.; Immirzi, A. *J. Am. Chem. Soc.* **1993**, *115*, 1160–1162.
(56) The thiazole- and imidazole-amine systems were developed and optimized at the same time. For synthetic and polymerization data for additional imidazole amine complexes, see refs 49,50.
(57) The synthesis and characterization of the trimethyl deviative of **15** is included in the Supporting Information.
(58) 75 °C data is shown for first generation systems, and 110 °C polymerization data is shown for second and third generation catalysts.
(59) Pangborn, A. K.; Giardello, M. A.; Grubbs, R. H.; Rosen, R. K.; Timmers, F. J. *Organometallics* **1996**, *15*, 1518.